Archives of Hydro-Engineering and Environmental Mechanics
Vol. 43 (1996), No. 1–4, pp. 59–77

Investigation of the Soil Phase Composition Below 0°C by Means of Differential Scanning Calorimetry

Tomasz Kozłowski

Kielce University of Technology, Al. 1000-lecia Państwa Polskiego 7, 25–314 Kielce, Poland

(Received February 24, 1997; revised April 15, 1997)

Abstract

Determining the unfrozen water content in a frozen soil-water system as a function of temperature is still a serious problem. Existing methods involve their own sets of assumptions and approximation, and a method giving the "real" soil phase composition as a function of temperature probably does not exist. The aim of the paper is to present a method able to construct the full curve of soil phase composition during a warming run of an individual sample from –28°C to +10°C, including such parameters of the process as the melting point and the non-freezable water content.

The method consists in determining the real heat flux function $q(T)$ absorbed by the frozen soil sample during the warming DSC (differential scanning colorimetry) run. It is based on searching for the distribution of "heat impulses" in relation to temperature, which convoluted with the apparatus function $a(T)$ gives a minimal deviation from the heat flux function $h(T)$ observed. The function $q(T)$ can easily be related to the function of unifrozen water content $u(T)$. The latter determines the important parameters of soil freezing process: the melting (or freezing) point T_0 and the content of "non-freezable" water u_n. Examples of computations and results are given.

Notation

$a(T)$ – apparatus function, 1/K,
c – thermal capacity, J/K,
C – specific heat, J/gK,
C_a – apparent specific heat of soil, J/gK,
F – field of phase change peak, J,
$f(T)$ – function of temperature,
f_i – content of fraction less than 2 μm, %,
$g(T)$ – calorimetric signal, J/K,
$h(T)$ – function of the phase change peak corrected in relation to the base line, J/K,

Δh – heat of phase change, mJ,
H, h – enthalpy, J/g, J,
I_P – plasticity index, %,
L – latent heat of phase change, J/g,
m – mass, g,
p/p_0 – relative vapour pressure,
$q(T)$ – exchanged heat as a function of temperature, J/K,
S – specific surface, m^2/g,
T – temperature, °C,
T_0 – melting of freezing point, °C,
T_L – initial temperature of peak, °C,
T_R – final temperature of peak, °C,
T_{SN} – temperature of spontaneous nucleation, °C,
u – content of unfrozen water, %,
u_n – content of nonfreezable water, %,
v – scanning rate, K/min, K/s,
w – water content, %,
w_{95} – water content at $p/p_0 = 0.95$, %,
w_L – liquid limit, %,
w_P – plasticity limit, %.

Subscripts

i – ice,
s – dry soil material,
u – unfrozen water,
w – water.

1. Introduction

It is widely known that a quantity of water in a frozen soil-water system remains unfrozen (Pietrzyk 1965, Anderson 1967, Anderson et al. 1978, Farouki 1986, Kozłowski 1995). A typical curve of the unfrozen water content is shown in Fig. 1. In the temperature interval $T > T_0$ ice is absent in the system and the unfrozen water content u equals the total water content w. On freezing, a supercooling down to the temperature of spontaneous nucleation T_{SN} is possible. At T_{SN} embryo nuclei form and grow to critical sizes, and crystallisation begins (Anderson 1968, Kozłowski 1989). As a result of the release of the latent heat L, the temperature of the system rises to the value of T_0, called the temperature of equilibrium

freezing (or freezing points). The phenomenon of supercooling enables one to determine the freezing point experimentally (Kozłowski 1990). Further extraction of heat leads to a lowering of temperature and successive freezing of the remaining unfrozen water according to the line AC in Fig. 1. However, for a given soil-water system at any temperature $T < T_0$, the unfrozen water content defined as

$$u = \frac{m_u}{m_s} 100 \tag{1}$$

is an accurate function of temperature ($u = f(T)$).

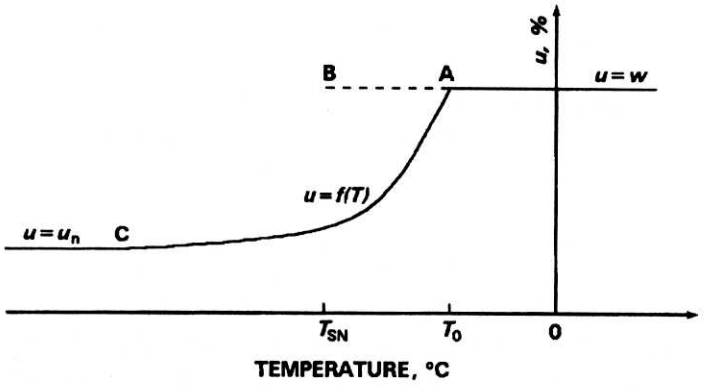

Fig. 1. The curve of unfrozen water content

It is often assumed that the unfrozen water content is independent of so-called thermal history (Frivik 1980). In other words, the unfrozen water according to the curve in Fig. 1 is the same both on the chilling and warming runs. So the temperature T_0, called the freezing point on chilling is called the melting point on warming. Of course, the non-equilibrium phenomena connected with supercooling occur only during the chilling run, this being the reason why the actual melting points has not yet been confirmed experimentally. One of the aims of the method presented is to obtain the melting point from experimental data.

Knowledge of the unfrozen water content function plays an important role in all thermal computations concerning soil freezing or thawing. This is connected with the concept of a so-called apparent specific heat of soil C_a.

Change of enthalpy of the system as a result of change of temperature along AC can be expressed as a sum of the normal component connected with heat capacity and a component connected with releasing or absorption of the latent heat:

$$dh = cdT + Ldm_u. \tag{2}$$

Differentiation of Eq. (2) with the assumption that the values of c and L are temperature independent gives the following equation:

$$\left(\frac{\delta h}{\delta T}\right)_p = c + L\left(\frac{\delta m_u}{\delta T}\right)_p . \tag{3}$$

Assuming that the soil heat capacity is the sum of capacities of the soil constituents (Low et al. 1968)

$$c = C_s m_s + C_u m_u + C_i m_i \tag{4}$$

and applying Eq. (1), gives

$$\left(\frac{\delta H}{\delta T}\right)_p = C_s + C_u \frac{u}{100} + C_i \frac{w-u}{100} + L\frac{\delta u}{\delta T} \tag{5}$$

where H is the enthalpy related to the mass of dry soil matrix.

In terms of thermodynamics the derivative on the left side of Eq. (5) expresses a form of specific heat, and is therefore called the apparent specific heat capacity of frozen soil:

$$C_a = C_s + C_u \frac{u}{100} + C_i \frac{w-u}{100} + L\frac{\delta u}{\delta T}. \tag{6}$$

Then the apparent specific heat C_a is the sum of appropriate terms for each of three frozen soil constituents, i.e. matrix, unfrozen water and ice, plus a term to account for the latent heat of phase change that is continually being given off or adsorbed. Eq. (6) is the base of thermal analysis of frozen ground. In the face of the extremely large value of the latent heat L (e.g. it is about 80 times greater than the specific heat of liquid water), the last term in Eq. (6) plays a very important part and cannot be neglected in any thermal computations.

Measurements of the unfrozen water contents in frozen soils have been made by dilatometry (Push 1978), adiabatic calorimetry (Kolaian and Low 1963, Pietrzyk 1964), isothermal calorimetry (Anderson and Tice 1971, 1973), x-ray diffraction (Anderson and Hoekstra 1966), nuclear magnetic resonanse (Tice et al. 1982, Kuyala 1989) and many other methods (vid. Kozłowski 1995). However, each involves its own set of assumptions and approximations and a method giving the "real" soil phase composition as a function temperature probably does not exist.

Determination of the function $u = f(T)$ was usually made by means of approximation of several points obtained in a series of experiments. Such a procedure is not very precise and cannot explain details of the freezing and thawing process. Only two new techniques, nuclear magnetic resonance NMR and differential scanning calorimetry DSC enable the monitoring of the continuous phase changes during freezing or thawing of individual soil samples.

The unfrozen water in frozen soil can be divided into two forms: so called non-freezable water u_n (Horiguchi 1985) and the water the quantity of which depends on temperature. The former does not freezes down to at least −30°C

(Anderson and Tice 1971) and its content can be successfully determined by the differential scanning calorimetry technique (DSC). Warming a soil sample from a low temperature of about −20°C gives an endothermic peak, the integration of which in relation to time or temperature determines the thermal effect connected with melting of ice contained in soil. The amount of the non-freezable water corresponds with the difference between the total amount of water and the amount of ice. However, problems appear while using the DSC technique to determine the unfrozen "freezable" water content. Beginning the calorimetric warming run from a temperature at which some quantity of the freezable water already exists (e.g. −5°C) makes it impossible to get the calorimetric base line fixed, because the phase transition of ice starts simultaneously with the scanning process. Therefore, the starting point of the warming run must be established possibly low, before the beginning of phase transitions. The curve of the unfrozen water content could be obtained by analysis of the whole of the warming endothermic peak recorded. Horiguchi (1985) gave an example of such an analysis. He assumed that the real thermal flux connected with the melting a quantity of ice in a small temperature interval ΔT_i corresponds with the part of the endothermic peak in this interval, and only with this part. Unfortunately, this assumption is not reasonable, even at low scanning rates about 0.1 K/min. Furthermore, the melting point of the sample, which is the parameter of particular importance, cannot be determine by that method. This paper presents a method for determining both the real unfrozen water curve and the melting point from the DSC data.

2. Outline of the DSC Technique

The principle of compensated scanning calorimeter is shown in Fig. 2. Two identical vessels, A with a sample and B without one, are located symmetrically inside calorimetric block K. Each vessel is equipped with an individual heat sensor and a micro-heater. The temperature of block T_K can be changed at a constant rate, called the scanning rate ν:

$$T_K = T_{K,0} + \nu t. \tag{7}$$

Because of the thermal flow between the block and the vessels, their temperatures T_A and T_B also changed, and there would occur identity

$$T_A = T_B = T_{init} + \nu t \tag{8}$$

in the case of absence of the sample in vessel A.

During experiments, the necessity of maintaining the condition (8) is the principle of operation of the calorimeter control unit. The presence of the investigated sample leads to a temperature difference between the vessels. On warming, temperature T_A remains behind temperature T_B because of a difference in thermal

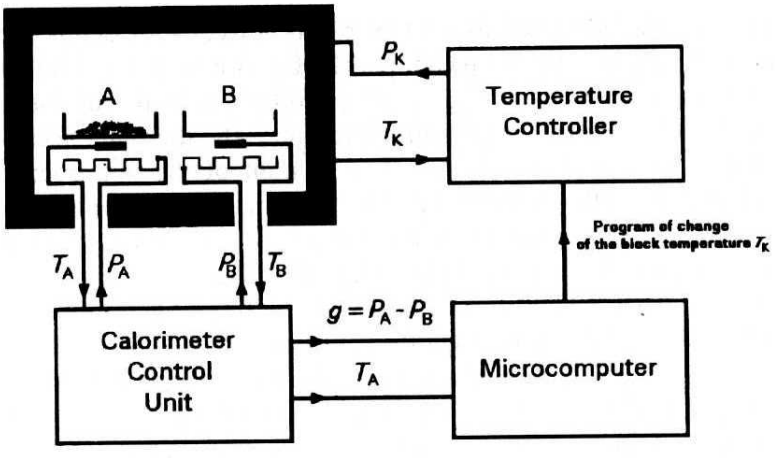

Fig. 2. Schematic diagram of the compensated scanning calorimeter

capacities. In this case, the calorimeter control unit supplies the heater A with an additional power g. It can be proved that the power g is proportional to the mass of the sample m, its specific heat C and the scanning rate:

$$g = Cmv. \tag{9}$$

The values of g recorded by a microcomputer as a function of current sample temperature are called the calorimetric signal $g(T)$. Because the specific heats of solids can be approximated by simple linear function, the plot of $g(t)$ in the temperature interval before the beginning of the phase transitions represents a straight line called the reference or base line. A phase change taking place in vessel A causes an increase of $g(T)$ in the case of the endothermic process of ice melting. It appears as a peak on the plot of the calorimetric signal. The field of the peak equals to the total heat of phase transition (or in other words – change of enthalpy of the system):

$$\Delta h = \int_{T_L}^{T_R} h(T)dT \tag{10}$$

where $h(T)$ is the function $g(T)$ corrected in relation to the base line and T_L and T_R are respectively the initial and final temperatures of the peak (Fig. 3).

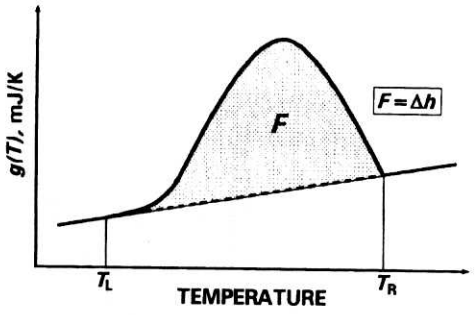

Fig. 3. Heat of phase change Δh as the field of peak on the calorimetric signal plot

3. Method of Determining the Phase Composition of Frozen Soil

3.1. Content of the Non-freezable Water

The whole peak recorded during a warming run from −28°C do +10°C can be attributed to phase change of all the ice contained in the soil sample:

$$m_i = \frac{\Delta h}{L}. \tag{11}$$

The content of the non-freezable water can be computed as the difference between the total water content and the ice content, which, after assuming Eq. (11), can be expressed as

$$u_n = w - \frac{100\Delta h}{Lm_s} \tag{12}$$

where Δh is the total heat of phase transition obtained according to Eq. (10).

3.2. The Unfrozen Water Content Curve and the Melting Point

Independent of the apparatus construction, thermograms obtained during the DSC run are not real thermal flux curves connected with the investigated process. Existence of thermal resistance between the sample and a heat sensor leads to an effect called broadening of the experimental curve (Hemminger and Höhne 1984). Let us analyse a thermal impulse connected with a phase transition of a crystalline substance. The impulse, in reality yielded at a strictly determined temperature T_0 called the melting or freezing point, is recorded as a peak, starting point alone of which is in T_0 and the width is an increasing function of the scanning rate (Fig. 4). More thermal impulses yield a peak being a superposition of a number of peaks (Fig. 5).

Normalisation of the function from Fig. 4 in relation to the total thermal effect Δh and the temperature T_0 gives an apparatus function $a(T)$ connected with the construction of a given calorimeter and being able to be estimated experimentally:

$$a(T_0 - T) = \frac{h(T_0 - t)}{\Delta h} \tag{13}$$

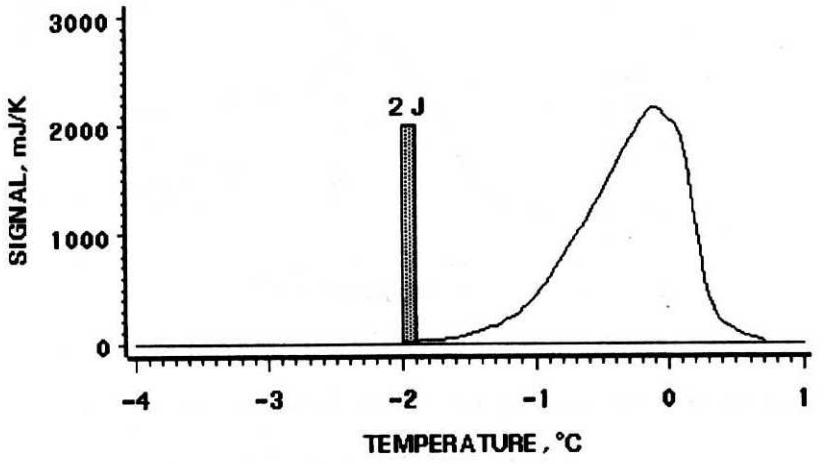

Fig. 4. Response of calorimeter to a single thermal impulse

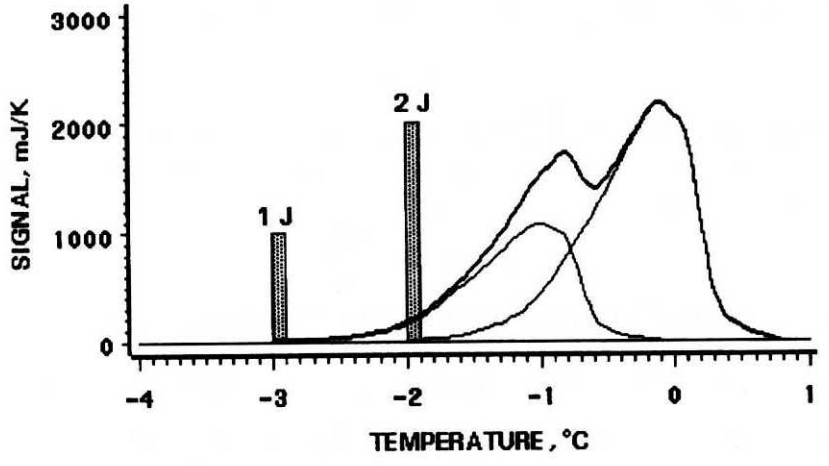

Fig. 5. Response of calorimeter to two thermal impulses as a superposition

where $h(T)$ is the observed heat flux thermogram, in J/K, and Δh is the total thermal effect absorbed or yielded at temperature T_0, in J.

In terms of mathematics, the observed function $h(T)$ is a convolution of the real function of thermal effects $q(T)$ and the apparatus function $a(T)$:

$$h(T) = \int_{-\infty}^{\infty} a(T - T')q(T')dT'. \tag{14}$$

Then, the problem of finding the real curve of heat flux consists in solving Eq. (14) in relation to $q(T)$ when the functions $h(T)$ and $a(T)$ are known. It is possible to solve the problem by use of the Fourier transforms, but the method is not always convergent. Thus the present writer decided to work out a method

based on a numerical analysis of the square deviations of the observed function $a(T)$ and convolution of the apparatus function $a(T)$ with functions $q_i(T)$, being successive approximation of the real function $q(T)$.

The observed function of heat flux $h(T)$ (or the calorimetric peak) was divided into a number of finite elements of width $\Delta T_i = T_{i+1} - T_i$, each with a constant value of thermal flux $h(T_i)$. It applied to the apparatus function $a(T)$ as well. Eq. (14) in the form of finite differences can be written as follow:

$$h(T_j) = \sum_{i=1}^{n} \sum_{j=i}^{i+m-1} a(T_j - T_i) q(T_i) \Delta T_i \tag{15}$$

when n is the number of elements of the observed function and l is the number of elements of the apparatus function.

A good approximation of the function $q(T_i)$ was determined by producing its possible forms $q_k(T_i)$, making their convolutions $h_k(T_i)$ with the apparatus function $a(T_i)$ according to Eq. (15), and analysing the following sums of square deviations:

$$D_k = \sum_{i=1}^{n} (h(T_i) - h_k(T_i))^2. \tag{16}$$

The value of D_k reaches minimum for the best approximation of $q(T_i)$.

The values of obtained real function of heat $q(T_i)$ multiplied by widths of the temperature intervals ΔT_i express a distribution of the conventional heat impulses attributed to the temperature intervals. The temperature of the last non-zero impulse is the temperature of the end of melting T_0 or the melting point, with an accuracy equal to the length of the temperature interval ΔT_i.

Now the values of the unfrozen water content function $u(T_i)$ can be calculated analogously to Eq. (12) as follows:

$$u(T_i) = w - \sum_{j=i}^{n} \frac{100 q(T_j) \Delta T_j}{L(T_j) m_s} \tag{17}$$

where $u(T_i)$ is the unfrozen water content at temperature T_i in percentages, $L(T_i)$ is the latent heat of fusion of ice at temperature T_i and m_s is the masss of dry soil in the sample, in g.

It is known that the value of L decreases with decreasing temperature. Horiguchi (1985) presented the following formula, obtained experimentally for water freezing on silica gels:

$$L(T) = 7.3T + 334. \tag{18}$$

Unfortunelly, the equation raises some questions. It is not clear to what extent the expected change of latent heat of water on the silica gels is caused either by the supercooling or by the alteration of structure of the bound water. Hence it

is hard to say whether Eq. (18) adequately expresses the latent heat of fusion of ice in a soil-water system. In this situation, the computations reported below were made assuming the constant value of the latent heat. The resulting error should be insignificant, as intensity of the phase changes decreases with temperature. Decreasing of $q(T_i)$ in Eq. (17) with temperature results in the influence of varying values of $L(T_i)$ also diminishing at lower temperatures. On the contrary, near 0°C the meaning of the assumed value of L is very great but now it is not expected to be very different from the constant value 334 J/g.

4. The DSC Experiment

4.1. Laboratory Equipment and Experimental Procedure

The Unipan-Thermal differential scanning calorimetry system Model 607 with an LN_2 colling system was used in the experiments. Basal parameters of the system are as follows:

- sensitivity: 5 mW to 180 mW,
- scanning rate: 0.1 K/min to 20 K/min,
- working temperature: −80°C to +400°C,
- noise level: $\leq$ 3 mJ/K at scanning rate 0.5 K/min.

A microcomputer was interfaced with the system for the scanning rate control and real-time data storage. Aluminium sample pans were weighed and filled with the soil pastes, sealed hermetically and weighed again. The masses of the soil samples were determined by differentiaion and numbered approximately 10 mg. A thin layer of the soil paste covered only the bottom of the pan which ensured very good exchange of heat. A quasi-uniform thermal field within the sample is a necessary condition of the method presented. The samples were cooled at a scanning rate of 1 K/min to −28°C and then warmed at a scanning rate of 0.5 K/min to +10°C at a calorimeter sensitivity of 5 mW. After experiments, pinholes were punched in the sample covers and the total water contents were determined by drying to constant mass at 110°C.

4.2. Material

For this study, sodium form of montmorillonite was used. The form had been obtained from natural bentonite from Chmielnik in Poland by repeated saturation of the less than 0.063 mm fraction and subsequent purifying from solutes by diffusion. The soil pastes were then dried at room temperature to a required total water content and stored in closed vessels for about three weeks before the experiment.

The soil properties were the following:

- plasticity limit: $w_P = 86.5\%$,
- liquid limit: $w_L = 253.7\%$,
- plasticity index: $I_p = 167.2\%$,
- fraction less than 2 μm: $f_i = 92\%$,
- water content at $p/p_0 = 0.95$: $w = 28.72\%$,
- external specific surface: $\bar{S} = 110$ m^2/g,
- total specific surface: $S = 644$ m^2/g,
- cation exchange capacity: C.E.C. = 111.12 mval/100 g of dry soil.

The total number of samples tested was $n = 28$.

4.3. Determining the Apparatus Function

The apparatus function $a(T)$ was determined on the basis of thermograms obtained by melting of six samples of pure ice with a scanning rate equal to 0.5 K/min. For the masses between 0.5 mg and 40 mg the observed shapes of peak were very similar. Error of determination of the melting point comprehended as the peak starting point was less than 0.1 K in all instances and error of determination of the latent heat was less than 1%. One of the peaks, obtained for a sample of 2.20 mg, was chosen for creation of the apparatus function. The main reasons for such a choice were excellent results obtained for this sample: the melting point $T_0 = +0.05$°C and the latent heat of fusion $L = 333.32$ J/g. The observed peak was divided into fields 0.1 K in width. The number of the fields, which corresponds with the value of l in Eq. (15), equalled 28. The area of each field was divided by the total field of the peak. Thus, the obtained apparatus function represents distribution of fractions of the total heat of fusion of ice at 0°C, which are observed at a wide temperature interval above an endothermic peak (Fig. 6).

4.4. Numerical Computations

Because of the difference between specific heats of solid and liquid phases of the same substance, the slopes of the base line before and after the peak are different in the main. Therefore, the peak $h(T)$ shown in Fig. 3 is usually determined in relation to a straight line connecting initial and final points of the phase transition (Figs. 7a,c). Such procedure would lead to a significant error in the case of very wide peaks associated with thawing of a moist soil sample. In the present investigation, for each investigated soil sample the obtained thermogram was referenced to the base line by a computer program taking into account the change in heat capacities of the sample constituents by the ice melting. The following method consisting in a "fluent" interpolation between the straight sections of the reference line before and after the interval of phase changes was used.

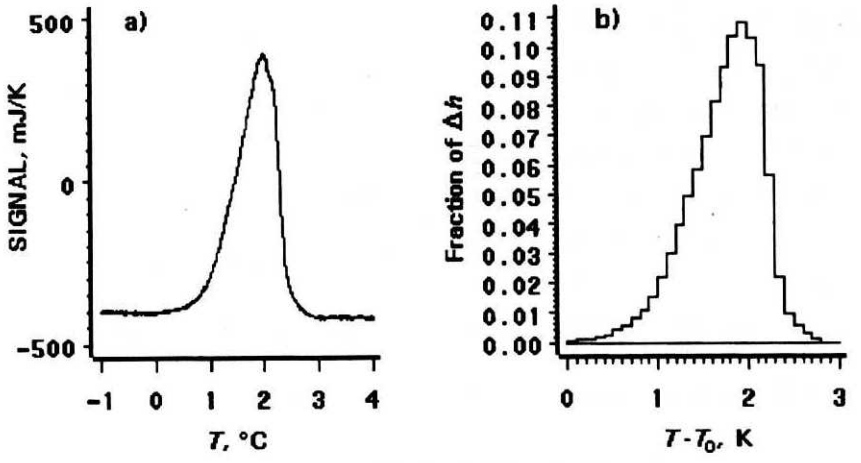

Fig. 6. The apparatus function: a) the initial corrected peak $h(T)$ recorded for a sample of pure ice; b) the apparatus function $a(T)$ determined exactly to one tenth of a Kelvin

Let the base line for temperatures $< T_L$ be expressed by the linear equation $g(T) = a_L T + b_L$ and for temperatures $> T_R$ – by $g(T) = a_R T + b_R$. Let us assume that the notional base line under the peak is expressed by the following quasi-linear equation:

$$\overline{g(T)} = a_S(T)T + b_S(T) \tag{19}$$

where $a_S(T)$ and $b_S(T)$ are temperature-dependent coefficients varying from a_L, b_L at temperature T_L to a_R, b_R at temperature T_R. The degree of this transformation depends on the phase change progress which expresses the following proportion:

$$\frac{a_L - a_R}{F} = \frac{a_L - a_S(T_i)}{\Delta F(T_i)} \tag{20}$$

where F is the field of all of the peak and $\Delta F(T_i)$ is the field of the part of the peak between temperatures T_L and T_i, both calculated in relation to $\overline{g(T)}$. Rearranging Eq. (2) gives

$$a_S(T_i) = a_L\left(1 - \frac{\Delta F(T_i)}{F}\right) + a_R\frac{\Delta F(T_i)}{F} \tag{21a}$$

and by analogy

$$b_S(T_i) = b_L\left(1 - \frac{\Delta F(T_i)}{F}\right) + b_R\frac{\Delta F(T_i)}{F}. \tag{21b}$$

The values of $a_S(T)$ and $b_S(T)$ were calculated by means of a recurrent method. The straight line mentioned above was the first approximation of the function $\overline{g(T)}$. In relation to this, the first approximation of $h(T)$ was determined as

$$h(T_i) = g(T_i) - \overline{g(T_i)} \tag{22}$$

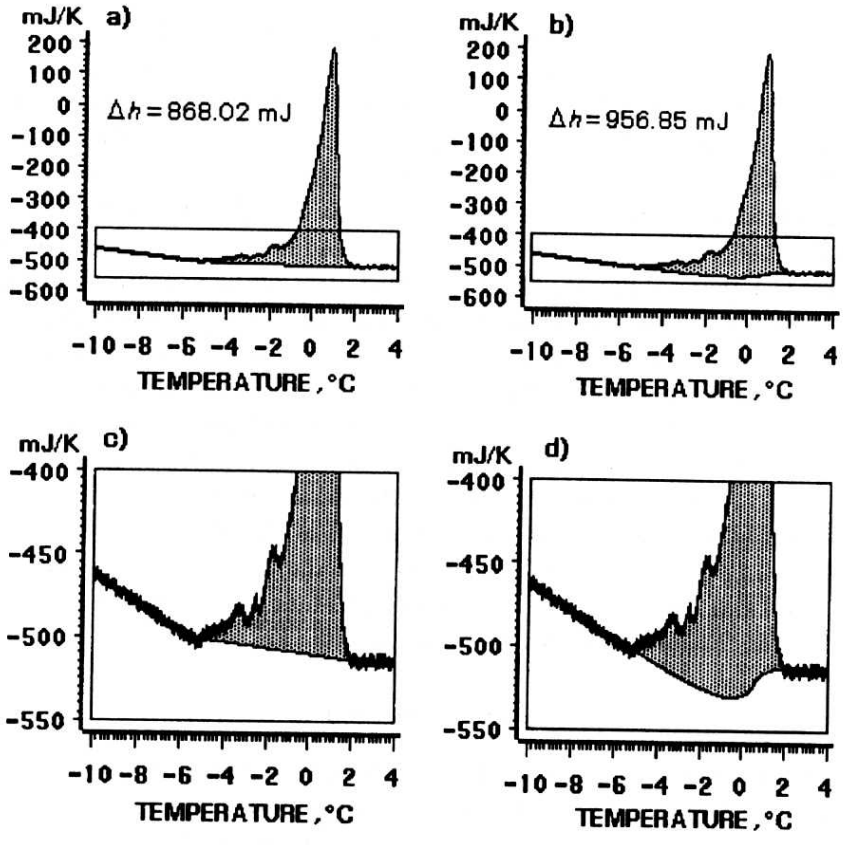

Fig. 7. Notional base line under the peak of phase change: a), c) straight line connecting beginning and final points of the phase transition; b), d) fluent base line determined taking into consideration change of specific heat during the process of phase transition

where $g(T)$ is the function of calorimetric sygnal in the temperature interval $[T_L; T_R]$. Next, the values of $\Delta F(T_i)$ were computed as

$$\Delta F(T_i) = \int_{T_L}^{T_i} h(T_i) dT. \tag{23}$$

Note that the same equation was used to calculate the value of F when $T_i = T_R$ and of course F corresponds to the total heat of phase change Δh according to Eq. (10).

Finally, the values of $a_S(T)$ and $b_S(T)$ were calculated in accordance with Eqs. (21ab). They were used to determine a new approximation of the notional base line according to Eq. (9) and the procedure started all over again. The procedure was terminated when the difference of two succesively determined values of F was less than an assumed value ε. In Figs. 7bd, this fluent notional base line calculated by use of the above method is shown.

The corrected peak $h(T)$ obtained was divided into n fields 0.1 K in width. A computer program calculated the total heat Δh of phase changes as the field of the peak (Eq. 10). Next, a form of the function $q_k(T_i)$ was created by an attribution of fractions of the total heat to temperatures T_i and dividing the fractions by $\Delta T_i = 0.1$ K. At successive stages of computations, elementary "bricks" of the fractions decreased from 20% of Δh to 0.625% od Δh. According to Eq. (15), the convolution of $q_k(T_i)$ with $a(T_i)$ was made and fitting was checked out by use of Eq. (16). A pass to another stage occurred after finding such a distribution of the fractions which gave a minimum of D_k. Unfortunately, such computations are time consuming and the program should create the successive forms of $q_k(T_i)$ in a reasonable manner (e.g. distribution with 60% od Δh attributed to temperature –12°C is impossible). The fact is that a computer with fast processor is needed. Finally, the function of unfrozen water content was computed in accordance with Eq. (17). The stages of transformation of the originally observed peak $h(T)$ into the unfrozen water content curve $u(T)$ is shown in Fig. 8.

The melting point T_0 is the temperature of the last non-zero impulse in the plot of $q(T)$ and the content of non-freezable water u_0 is obtained according to Eq. (12) or as the last value of differences in Eq. (17).

4.5. Discussion

The thawing process. Analyzis of the real heat flux thermonograms like this in Fig. 8 suggests that the process of the ice melting in the soil-water system is not a continuous phase change. Absorption of the heat occurs at distinct temperature intervals and it is not strictly an increasing function of temperature. Therefore, the apparent specific heat capacity obtaining by differentiation of a continuous unfrozen water function is only an approximation. All obtained thermonograms $q(T)$, not reproduced here, have shown the interval of vanishing of the phase effects before the final intensive impulses near melting point. This is the cause of the occurrence of the characteristics plateau on the unfrozen water curve (Figs. 9). Results reported by Anderson & Tice (1973) for freezing processes indicate an effect of two interfacial domains, which agree with the present data for thawing processes though one can probably speak about not less than three such domains. Finally, the results do not confirm the S-shape of the $u(T)$ curve near the melting point reported by Kuyala (1989). Probably too large samples used in his NMR investigation could not ensure the quasi-uniform heat field, which generally refers to most of phase composition researches and leads to "blurring" of results.

A typical curve of the unfrozen water content obtained as a result of these experiments is shown in Fig. 10. One can distinguish individual "stages" of change in phase composition, particularly a specific plateau CD near the melting point. Mean intensity of phase changes on stage BC numbers $\Delta u/\Delta T = 2.8\%$/K and on the final stage DE – 95%/K (about 34 times higher).

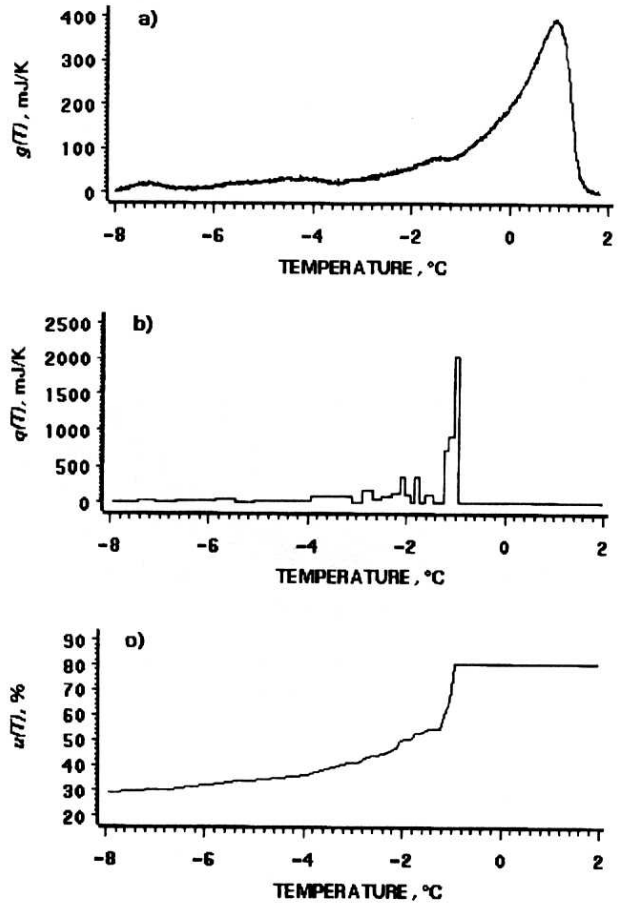

Fig. 8. An example of transformation of the observed peak into the unfrozen water content curve: a) initial peak $h(T)$ corrected in relation to the fluent base line; b) the thermogram of real thermal effects $q(T)$; c) the unfrozen water content curve

An effect of the latent heat function $L(T)$. Two unfrozen water curves shown in Fig. 10 were obtained for the same sample by use of Eq. (17) accepting either constant value of L or functional relationship according to Eq. (18). The difference is not significant. Because it increases with decreasing temperature, the greatest differences occur for the non-freezable water content u_0. In the case of calcium bentonite, the mean value of the difference between $u_{n,L=const}$ and $u_{n,L=L(T)}$ was 0.79% in relation to the soil dry mass m_S, which constituted about 2.5% of the mean non-freezable water content equal to 32.06%. In order words, the relative error connected with acceptance of the constant value of L does not exceed 2.5%.

The non-freezable water content. In all samples investigated the contents of non-freezable water u_n was not less than the water content at relative vapour pressure $p/p_0 = 0.95$. However, the data indicate the characteristic minimum

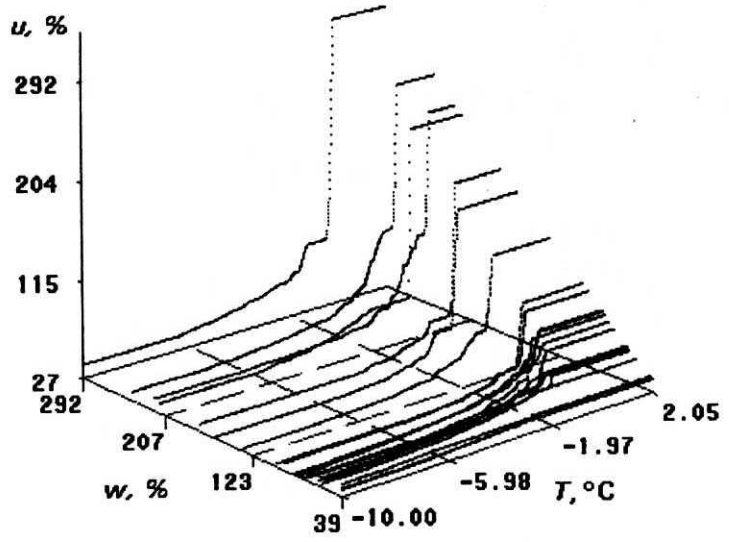

Fig. 9. Curves of the unfrozen water content u obtained for sodium bentonite at different total water contents w

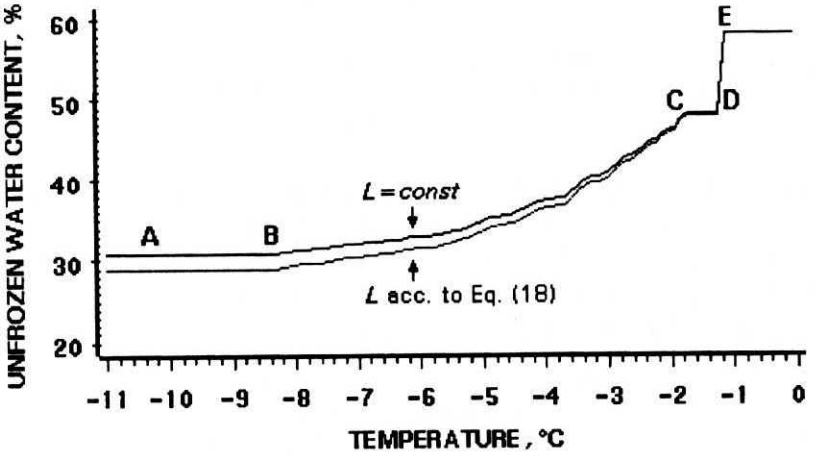

Fig. 10. Curves of the unfrozen water content for the same sample, determined assuming either the constant value of latent heat L or the functional relationship according to Eq. (18)

on curve of u_n vs. the total water content w (Fig. 11), the explanation of which probably requires the assuming of a complicated superposition of such factors as the interlamellar swelling (increases with increasing w) and presence of small quantities of supercooled water in some micro-pores (increases with decreasing w). The data will be reported elsewhere. Some samples with very low total water contents did not show any phase effects; for them of course $u = u_n = w$.

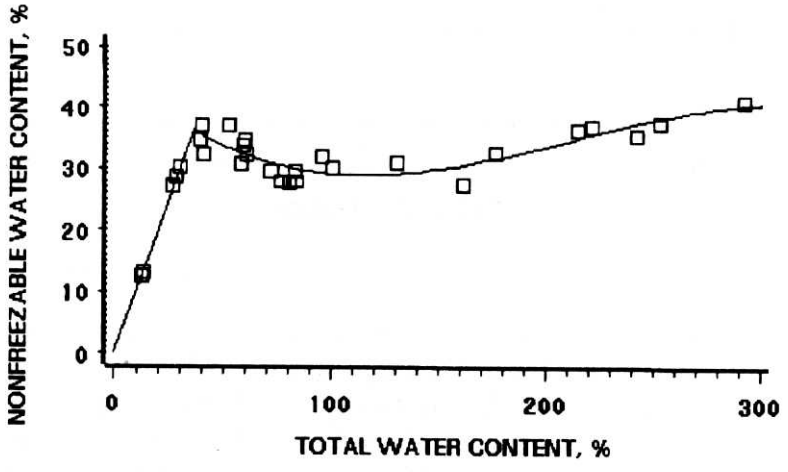

Fig. 11. The content of non-freezable water u_n as a function of total water content w (Na bentonite)

The melting point. The melting point T_0 is an increasing function of total water content w (Fig. 12) which conform with theoretical (Low et al. 1968) and semi-empirical (Kozłowski 1994) relationships for freezing point depression. It should be stressed that the presented experimental method is the first enabling one to determine the melting point precisely. Other recently reported methods, both based on NMR and DSC techniques, were not able to measure this very important parameter of the process (Yong et al. 1978, Tice et al. 1982, Horiguchi 1985, Kuyala 1989). The results obtained may confirm the thesis that thermal history does not play an important role in the freezing-thawing of the soil water system. Further experiments comparing does not seem to be very significant in the light if the present experiment.

5. Conclusions

A method for constructing the real unfrozen water curve and determining the melting point from the DSC data has been presented. The method consists in determining the real heat fluz function $q(T)$ absorbed by the frozen soil sample during the warming DSC run. It is based on searching for a distribution of "heat impulses" in relation to temperature, which convoluted with the apparatus function $a(T)$ gives a minimal deviation from the observed heat flux function $h(T)$.

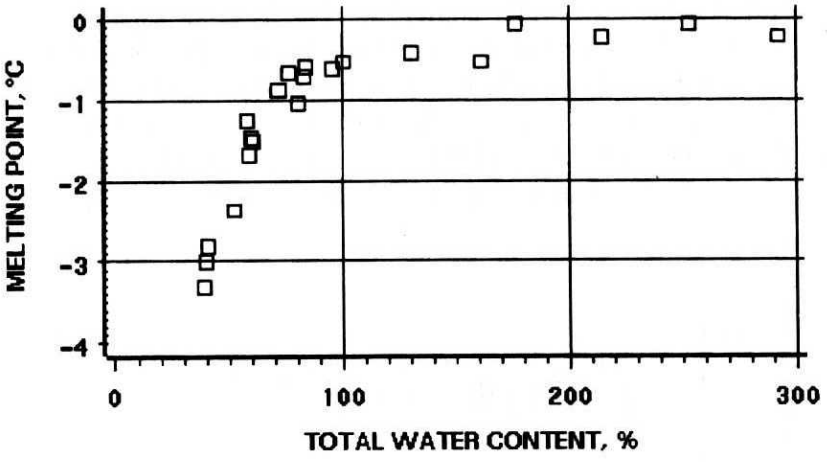

Fig. 12. The melting point T_0 as a function of total water content w (Na bentonite)

The function $q(T)$ can be easily related to the function of unfrozen water content $u(T)$. The latter determines the important parameters of the soil freezing process: the melting (or freezing) point T_0 and the content of "non-freezable" water u_n.

The presented exemplary results obtained for sodium montmorillonite speaks in favour of the method. It seems to be precise enough to investigate e.g. the influence of total water content on the content of non-freezable water and the melting point. The possibility of using very small samples with a quasi-uniform temperature field has led to the obtaining of new interesting data about the melting process which proved not to be a continuous phase change. The absorption of the heat occurs at distinct temperature intervals and it is not a strictly increasing function of temperature. Besides, all the obtained curves of unfrozen water content showed a characteristic plateau near the melting point, about 1–2 K in width. This is connected with the temporary vanishing of phase changes.

Further investigations will supply evidence as to whether the conclusions presented above are useful for soils of different mineral and cation complex composition.

References

Anderson D. M. (1967): The interface between ice and silicate surfaces, *J. Coll. Interface Sc.*, 25.

Anderson D. M. (1968): Undercooling, freezing point depression, and ice nucleation of soil water, *Israel J. Chem.*, 6.

Anderson D. M., Hoekstra P. (1965): Migration of interlamellar water during freezing and thawing of Wyoming bentonite, *Soil Sc. Soc. Am. Proc.*, 35.

Anderson D. M., Push R., Penner E. (1978): *Physical and thermal properties of frozen ground*, In: *Geotechnical Engineering for Cold Regions*, McGraw-Hill.

Anderson D. M., Tice A. R. (1971): Low temperature phases of interfacial water in clay-water systems, *Soil Sc. Soc. Am. Proc.*, 35.

Anderzon D. M., Tice A. R. (1973): The unfrozen interfacial phase in frozen soil water systems, *Ecol. Stud.*, 4.

Farouki O. T. (1986): *Thermal Properties of Soils*, Trans Tech. Pub., Clausthal-Zellerfeld.

Frivik P. E. (1982): *State-of-the-art report. Ground freezing: thermal properties, modeling of processes and thermal design*, Selected Papers of the 2nd Int. Symp. on Ground Freezing, Elsevier Sc. Pub. Co., Amsterdam.

Hemminger W., Höhne G. (1984): *Calorimetry. Fundamentals and Practice*, Verlag Chemie GmbH.

Horiguchi K. (1985); Determination of unfrozen water content by DSC, Proc. 4^{th} Int. Symp. Ground Freezing, Sapporo, Vol. 1, A. A. Balkema, Rotterdam.

Kolaian J. H., Low P. F. (1963): Calorimetric determination of unfrozen water in montmorillonite pastes, Soil Sc., 95.

Kozłowski T. (1989): Investigation of the supercooling in clayey soils, In: *Frost in Geotechnical Engineering*, VTT Symposium 94, Vol. 1, Espoo.

Kozłowski T. (1990): Badania obniżenia punktu zamarzania wody w wybranych gruntach modelowych, *Archiwum Hydrotechniki*, Vol. 37, 1–2.

Kozłowski T. (1994): Freezing point of soil water as a function of mineral composition and physical properties, *Archives of Hydro-Engineering and Environmental Mechanics*, Vol. 41, 3–4.

Kozłowski T. (1995): Influence of the total water content on the unfrozen water content below 0°C in model soils, *Archives of Hydro-Engineering and Environmental Mechanics*, Vol. 41, 3–4.

Kuyala K. (1989): Unfrozen water of Finnish soils measured by NMR, *Proc. Frost in geotechnical engineerin*, VTT Symposium 94, Espoo.

Low P. F., Anderson D. M., Hoekstra P. (1968): Some thermodynamic relationships for soils at or below the freezing point, *Water Resour. Res.*, 4.

Pietrzyk K. (1976): Metoda określania zawartości wody niezamarzniętej w gruncie zamarzającym, *Drogownictwo*, 12.

Push R. (1979): Unfrozen water as a function of clay microstructure, *Proc. 1st Symp. Ground Freezing*, Elsevier Sci. Pub. Comp., Amsterdam.

Tice A. R. et al. (1982): Unfrozen water contents of submarine permafrost by nuclear magnetic resonance, *Selected Papers of 2nd Int. Symp. On Ground Freezing*, Elsevier Sc. Pub. Co., Amsterdam.

Yong R. N. et al. (1978): Prediction of salt influence on unfrozen water content in frozen soils, *Proc. 1st Int. Symp. Ground Freezing*, Elsevier Sci, Pub. Comp., Amsterdam.